

# Time-resolved probing of the ground state coherence in rubidium

Martin Oberst,<sup>1,\*</sup> Frank Vewinger,<sup>2,3</sup> and A. I. Lvovsky<sup>2</sup>

<sup>1</sup>Fachbereich Physik, Universität Kaiserslautern, 67653 Kaiserslautern, Germany

<sup>2</sup>Institute for Quantum Information Science, University of Calgary, Alberta T2N 1N4, Canada

<sup>3</sup>Present address, Institut für Angewandte Physik, Universität Bonn, Wegelerstrasse 8, 53115 Bonn, Germany

\*Corresponding author: oberst@physik.uni-kl.de

Received January 25, 2007; revised April 4, 2007; accepted April 24, 2007;  
posted May 1, 2007 (Doc. ID 79385); published June 13, 2007

We demonstrate the preparation and probing of the coherence between the hyperfine ground states  $|5S_{1/2}, F=1\rangle$  and  $|5S_{1/2}, F=2\rangle$  of the  $^{87}\text{Rb}$  isotope. The effects of various coherence control techniques, i.e., fractional stimulated Raman adiabatic passage and coherent population return, on the coherence are investigated. These techniques are implemented using nearly degenerate pump and Stokes lasers at 795 nm (Rb  $D1$  transition), which couple the two hyperfine ground states via the excited state  $|5P_{1/2}, F=1\rangle$  through a resonant two-photon process in which a coherent superposition of the two hyperfine ground states is established. The medium is probed by an additional weak laser, which generates a four-wave mixing signal proportional to the ground state coherence and allows us to monitor its evolution in time. The experimental data are compared with numerical simulations. © 2007 Optical Society of America

OCIS codes: 190.4380, 190.2620, 190.1900, 270.1670, 300.6210.

The techniques of stimulated Raman adiabatic passage (STIRAP) [1] and coherent population return (CPR) [2] are of importance in various fields of physics. STIRAP is used for, e.g., coherent control of population transfer [1] between atomic levels, preparing coherent superposition states [3], efficient generation of terahertz radiation [4], and probing atom–photon entanglement [5]. Coherent population transfer helps to enhance frequency conversion processes [6,7], generate attosecond pulses [8–13], and improve the resolution of spectroscopic measurements [14]. Most investigations of these techniques have so far concentrated on the dynamics of population of various energy levels in the system but never on the coherence between them. At the same time, coherence is an essential element of these processes, and it is important to develop a technique for its time-resolved measurement. The present Letter achieves this goal.

In this work we prepare and probe the coherence between the two hyperfine ground states  $|5S_{1/2}, F=1\rangle$  and  $|5S_{1/2}, F=2\rangle$  in the  $^{87}\text{Rb}$  isotope. We perform, for the first time to our knowledge, a detailed study of two coherence manipulation techniques, namely, fractional STIRAP [15] and CPR. For both of these processes, the temporal evolution of the coherence is investigated and compared with numerical simulations. We also demonstrate that the efficiency of four-wave mixing in these systems depends on the generated coherence and not on the instantaneous electric fields.

Both schemes use two laser fields, referred to as the pump and Stokes fields, which resonantly couple the hyperfine state  $|1\rangle$  ( $5S_{1/2}, F=1$ ) of  $^{87}\text{Rb}$  to an intermediate state  $|2\rangle$  ( $5P_{1/2}, F=1$ ) and state  $|2\rangle$  to the target state  $|3\rangle$  ( $5S_{1/2}, F=2$ ) in a  $\Lambda$ -type energy level configuration (Fig. 1). Neglecting decoherence, the coupling creates a (transient or permanent) coherent superposition between states  $|1\rangle$  and  $|3\rangle$ , the so-called dark state [1] of the system:

$$|ds\rangle = \cos \theta(t)|1\rangle - \sin \theta(t)|3\rangle, \quad (1)$$

where the mixing angle  $\theta(t)$  is determined by

$$\tan \theta(t) = \Omega_P(t)/\Omega_S(t), \quad (2)$$

with  $\Omega_{P,S}$  being the Rabi frequencies of the pump and Stokes lasers.

The coherence between states  $|1\rangle$  and  $|3\rangle$  is defined as the off-diagonal element  $\rho_{13}$  of the system's density matrix. According to Eq. (1), it is given by

$$\rho_{13}(t) = \cos \theta(t) \sin \theta(t) \quad (3)$$

and thus is fully determined by the temporal evolution of the Rabi frequencies  $\Omega_P$  and  $\Omega_S$ . For fractional STIRAP, the pump and Stokes lasers are pulsed, exciting the medium in a counterintuitive order; i.e., the Stokes laser precedes the pump. At the moment  $t=t_f$  both lasers are simultaneously, adiabatically turned off, resulting in constant ratio (2) for  $t>t_f$ . Any coherence  $\rho_{13}$  prepared prior to  $t=t_f$  will then stay in the system even after the termination of the driving fields [15], gradually dephasing at the ground state decoherence rate [16].

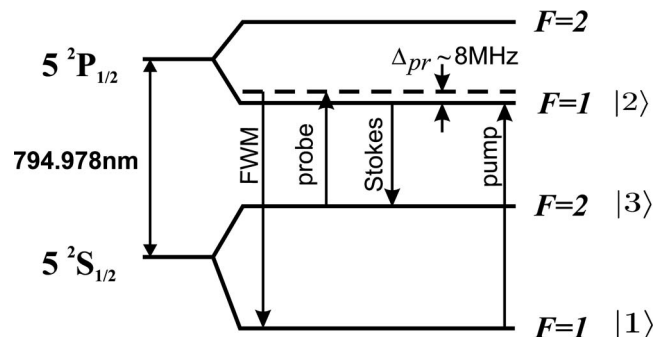


Fig. 1. Coupling scheme for the preparation and probing of the coherence  $\rho_{13}$  in  $^{87}\text{Rb}$ . The hyperfine splittings and detunings are exaggerated for clarity.

The second technique used to prepare coherence  $\rho_{13}$  is coherent population return. Here the pump field is continuous ( $\Omega_P = \text{constant}$ ) and the Stokes laser is pulsed with a Gaussian shape, so  $\Omega_S(t)$  is time dependent. The atomic population, initially in state  $|3\rangle$ , is transferred to state  $|1\rangle$  and back again as the Stokes field is applied, resulting in a transient coherence between the two states.

The ground state coherence is probed by an additional weak laser field, which induces a four-wave mixing (FWM) signal close to the pump laser wavelength at 795 nm (Fig. 1). Assuming perfect phase matching and neglecting depletion, absorption, and losses, which is justified for the optical densities used, the propagation of the FWM field is given by

$$\left| \frac{\partial E_{\text{FWM}}}{\partial z} \right| = \frac{\pi N \omega_{\text{FWM}} \mu_{12} \mu_{23}}{\hbar c \epsilon_0 \Delta_{\text{pr}}} |\rho_{13}| |E_{\text{pr}}|. \quad (4)$$

Here  $N$  denotes the number density of the sample,  $\mu_{23}$  and  $\mu_{12}$  are the dipole moments for the corresponding transitions,  $E_{\text{pr}}$  is the probe field amplitude, and  $\Delta_{\text{pr}}$  is the detuning of the probe field from the transition  $|2\rangle \rightarrow |3\rangle$ . All fields are assumed to propagate in the positive  $z$  direction. Equation (4) shows that the electric field of the FWM radiation at frequency  $\omega_{\text{FWM}}$  is proportional to the coherence  $|\rho_{13}|$  and can serve to measure the latter.

The experiments are carried out in a 5 cm long Rb vapor cell with 13 hpa of neon as a buffer gas. The temperature of the Rb vapor is 60°C, which corresponds to a number density of the order of  $10^{11} \text{ cm}^{-3}$ . The pump field is generated by a continuous Ti:sapphire laser (Coherent MBR-110) with a narrow spectral linewidth ( $\sim 100$  kHz). The Stokes and probe fields are both provided by a continuous diode laser (Toptica DLL100), which is frequency locked to the Ti:sapphire laser at the 6.8 GHz Rb hyperfine splitting of the  $|5^2S_{1/2}\rangle$  state with a precision of better than 10 Hz. The output of the diode laser is split into the Stokes and probe beams via a combination of a  $\lambda/2$  wave plate and a polarizing beam splitter.

All three beams are sent through acousto-optical modulators, which allows control over the temporal shape, frequency, and relative position of the different pulses in time. We employ the single-pass configuration for the Stokes and probe fields, resulting in frequency shifts of 80 and 88 MHz, respectively, and the double-pass configuration for the pump, leading to a 160 MHz shift. The three beams with diameters (FWHM) of  $\varnothing_P = 1.26$  mm,  $\varnothing_S = 1.76$  mm, and  $\varnothing_{\text{pr}} = 0.76$  mm for pump, Stokes, and probe, respectively, are then overlapped and directed into the Rb vapor cell located in a magnetically shielded oven. The polarizations of the probe laser and the generated FWM signal are orthogonal to the pump and Stokes lasers.

After the cell, the FWM signal and the probe laser are separated from the other fields by using a polarizer and are overlapped with the unmodulated output of the Ti:sapphire laser on a fast photodiode for heterodyne detection. The beat signal proportional to the

electric field of the FWM signal is monitored as a function of time by using a spectrum analyzer with a 200 ns resolution.

For fractional STIRAP to work, the population has to be transferred to state  $|1\rangle$  at the beginning of the process. This is realized by optical pumping with the leading part of the Stokes pulse, which exceeds the duration of the pump pulse by more than 1 order of magnitude ( $\tau_S \approx 24 \mu\text{s}$  and  $\tau_P \approx 2 \mu\text{s}$ , respectively, FWHM of intensity); see Fig. 2. The probe laser is pulsed with a pulse duration of  $\tau_{\text{pr}} = 500$  ns (FWHM of intensity). Typical powers are of the order of several milliwatts for the pump and Stokes radiation and a few hundred microwatts for the probe laser. We verified that the probe laser does not significantly influence the coherence by checking that the FWM intensity is proportional to that of the probe. With the pulse parameters given, we estimate the Rabi frequencies to be of the order of  $\Omega_P = 0.09 \text{ ns}^{-1}$ ,  $\Omega_S = 0.12 \text{ ns}^{-1}$ , and  $\Omega_{\text{pr}} = 0.08 \text{ ns}^{-1}$  for the pump, Stokes, and probe lasers.

To measure the coherence  $\rho_{13}$ , the delay  $\Delta\tau_{\text{pr}}$  of the probe pulse with respect to the pump and Stokes pulses is varied in  $0.2 \mu\text{s}$  steps, and the FWM signal is detected. Figure 2 shows the time dependence of the FWM radiation and therefore the temporal evolution of the prepared coherence  $|\rho_{13}|$  in the system.

The presence of coherence and FWM after the excitation lasers have been turned off contrasts with the classically expected behavior of FWM, where the created field is proportional to the product of the three fields irradiated on the medium,  $E_{\text{FWM}} \propto E_S E_P E_{\text{pr}}$ . This residual coherence  $\rho_{13}$  is a signature of fractional STIRAP [15], since only a part of the population is transferred from state  $|1\rangle$  to state  $|3\rangle$  during the interaction with pump and Stokes laser pulses. Upon termination of the excitation pulses, the signal experiences exponential decay due to decoherence [16]. We found the decay constant to equal  $20 \mu\text{s}$ , which is slightly longer than the  $15 \mu\text{s}$  expected from diffusion out of the beam [17].

For the CPR experiment, the system is prepared in state  $|3\rangle$  by means of optical pumping via a continuous pump laser with a Rabi frequency of  $\Omega_P \approx 0.028 \text{ ns}^{-1}$  (as determined from the beam param-

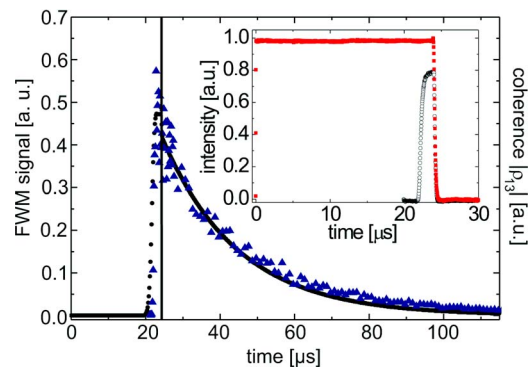


Fig. 2. (Color online) Fractional STIRAP process: FWM signal as a function of the probe laser delay  $\Delta\tau_{\text{pr}}$  (triangles) and numerical simulation (filled circles). Inset, temporal shape of the pump (open circles) and Stokes pulses (filled rectangles).

eters). The Stokes laser is pulsed with a Gaussian pulse shape of a  $\tau_S=25.5\ \mu\text{s}$  duration (FWHM of Rabi frequency). We perform several experimental runs with different Stokes field intensities. The probe laser is provided as continuous radiation with  $\Omega_{\text{pr}}\approx 0.006\ \text{ns}^{-1}$  (as determined from the beam parameters). The continuous probe laser provides real-time information on the evolution of coherence. As in the previous case, the probe laser does not significantly influence the prepared coherence.

Figure 3(a) shows the measured FWM signal as a function of the Stokes Rabi frequency. This result is in good agreement with the numerically calculated time evolution of the coherence  $|\rho_{13}|$  [Fig. 3(b)]. The proportionality coefficient between the Stokes Rabi frequency  $\Omega_S$  and the square root of the laser power  $P$ , given by  $182\ \text{MHz}/\sqrt{W}$  retrieved from the fit, is 1.3 times lower than the value expected from our beam parameters. The discrepancy present in the raising edges of the curves is due to absorption of the Stokes laser in the vapor cell.

Again, the signal observed in the CPR experiment shows significantly nonclassical behavior. Whereas a classical FWM should be proportional to the Stokes field, the signal measured at  $\Omega_S > \Omega_P$  exhibits a minimum when the Stokes field is maximized. This is easily understood: according to Eq. (3), the maximum co-

herence is reached when  $\Omega_S(t)=\Omega_P$  and both levels  $|1\rangle$  and  $|3\rangle$  are equally populated. If the Stokes Rabi frequency increases above that of the pump, and thus  $\theta$  falls below  $45^\circ$ , the coherence is reduced, as more than half of the population is transferred to state  $|1\rangle$ . This behavior is clearly displayed by the experimental observation, Fig. 3.

We have demonstrated the preparation of the ground state coherence in Rb vapor via fractional STIRAP and CPR and the detection of this coherence by FWM. The experimental results fit very well with numerical simulations and give clear evidence for the nonclassical character of these coherence control techniques. The presented method provides a powerful tool for the preparation and probing of coherence in a variety of systems.

We acknowledge valuable discussions with K. Bergmann, T. Halfmann, and E. Figueroa and thank J. Appel for assistance with the laser system. The work was funded by the Deutsche Forschungsgemeinschaft (Graduiertenkolleg 792), Alberta Ingenuity Fund, Canada Foundation for Innovation, and Canadian Institute for Advanced Research, Natural Sciences and Engineering Research Council of Canada, and QuantumWorks.

## References

1. N. V. Vitanov, T. Halfmann, B. W. Shore, and K. Bergmann, *Annu. Rev. Phys. Chem.* **52**, 764 (2001).
2. M. Jain and S. E. Harris, *Opt. Lett.* **22**, 636 (1997).
3. F. Vewinger, M. Heinz, R. Garcia-Fernandez, N. V. Vitanov, and K. Bergmann, *Phys. Rev. Lett.* **91**, 213001 (2003).
4. N. G. Kalugin and Y. V. Rostovtsev, *Opt. Lett.* **31**, 969 (2006).
5. J. Volz, M. Weber, D. Schlenk, W. Rosenfeld, J. Vrana, K. Sauke, C. Kurtsiefer, and H. Weinfurter, *Phys. Rev. Lett.* **96**, 030404 (2006).
6. A. J. Merriam, S. J. Sharpe, H. Xia, D. Manuszak, G. Y. Yin, and S. E. Harris, *Opt. Lett.* **24**, 625 (2001).
7. M. Jain, H. Xia, G. Y. Yin, A. J. Merriam, and S. E. Harris, *Phys. Rev. Lett.* **77**, 4326 (1996).
8. S. E. Harris and A. V. Sokolov, *Phys. Rev. A* **55**, R4019 (1997).
9. A. V. Sokolov, D. R. Walker, D. D. Yavuz, G. Y. Yin, and S. E. Harris, *Phys. Rev. Lett.* **85**, 562 (2000).
10. A. V. Sokolov, D. D. Yavuz, D. R. Walker, G. Y. Yin, and S. E. Harris, *Phys. Rev. A* **63**, 051801 (2001).
11. S. E. Harris and A. V. Sokolov, *Phys. Rev. Lett.* **81**, 2894 (1998).
12. A. V. Sokolov, D. D. Yavuz, and S. E. Harris, *Opt. Lett.* **24**, 557 (1999).
13. D. D. Yavuz, A. V. Sokolov, and S. E. Harris, *Phys. Rev. Lett.* **84**, 75 (2000).
14. T. Halfmann, T. Rickes, N. V. Vitanov, and K. Bergmann, *Opt. Commun.* **220**, 353 (2003).
15. N. V. Vitanov, K. A. Suominen, and B. W. Shore, *J. Phys. B* **32**, 4535 (1999).
16. E. Figueroa, F. Vewinger, J. Appel, and A. I. Lvovsky, *Opt. Lett.* **31**, 2625 (2006).
17. F. A. Franz and C. Volk, *Phys. Rev. A* **14**, 1711 (1976).

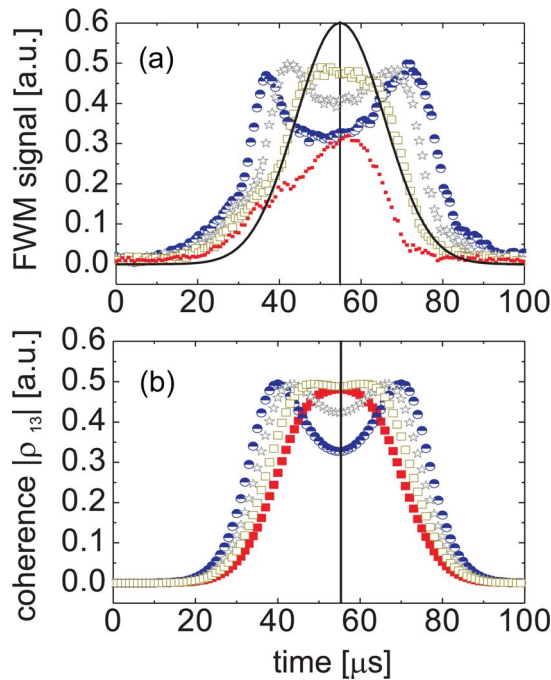


Fig. 3. (Color online) Coherence during the CPR process: (a) measured FWM signal and (b) calculated coherence  $|\rho_{13}|$  for different Stokes pulse intensities. The maximum Stokes Rabi frequencies (at  $t=54.9\ \mu\text{s}$ ) are  $\Omega_S=0.023\ \text{ns}^{-1}$  (filled rectangles);  $\Omega_S=0.033\ \text{ns}^{-1}$  (open rectangles);  $\Omega_S=0.05\ \text{ns}^{-1}$  (stars);  $\Omega_S=0.075\ \text{ns}^{-1}$  (half-filled circles). The solid curve in (a) shows the temporal profile of the Stokes Rabi frequency (scale in arbitrary units).